Cathode Coupling in Hall Thrusters

IEPC-2007-278

Presented at the 30th International Electric Propulsion Conference, Florence, Italy
September17 – 20, 2007

Kristina K. Jameson[*], Dan M. Goebel[†], Richard R. Hofer[‡], and Ron M. Watkins[§]
Jet Propulsion Laboratory, California Institute of Technology, Pasadena, CA 91109

Abstract: The effects of cathode flow rate and cathode coupling on total thruster efficiency are examined for a 6 kW Hall thruster. The thruster was operated with a traditionally mounted external cathode and its performance and efficiency are compared to its operation with an internally-mounted, on-axis cathode. To analyze the efficiency at different operating conditions, several external diagnostics were employed. The diagnostics include a thrust stand, far-field probes (emissive, Faraday, ExB, and RPA), near-field probes (Langmuir and emissive), calibrated mass flow rate meters, and calibrated voltage and current measurements. The cathode to ground coupling voltage decreased significantly (approximately 6-10 V) when using the internally mounted cathode compared to the externally mounted cathode for a given power level. In addition, the cathode to ground coupling voltage was observed to increase in magnitude with decreasing cathode flow rate at a constant power level but the total thruster efficiency was not affected. Lastly, the total thruster efficiency was improved by 2-3% when utilizing the internal cathode versus the external cathode.

Nomenclature

A	=	probe area
e	=	electron charge
F_t	=	thrust vector correction factor
I	=	probe current
I_b	=	ion beam current
I_d	=	discharge current
I^+	=	single ion current
I^{++}	=	double ion current
I^{+++}	=	triple ion current
k	=	Boltzman's constant
M	=	ion mass
m	=	electron mass
$\dot{m}_a$	=	anode mass flow rate
$\dot{m}_b$	=	ion beam mass flow rate
$\dot{m}_c$	=	cathode mass flow rate
$\dot{m}_t$	=	total mass flow rate

[*] APT Staff, Electric Propulsion Group, Kristina.K.Jameson@jpl.nasa.gov.
[†] Senior Research Scientist, Propulsion and Materials Engineering Section, Dan.M.Goebel@jpl.nasa.gov.
[‡] Technical Staff Member, Electric Propulsion Group, Richard.R.Hofer@jpl.nasa.gov.
[§] Engineering Staff Member, Electric Propulsion Group, Ron.M.Watkins@jpl.nasa.gov.

n = plasma density
P_{aux} = auxiliary power
P_d = discharge power
P_{ext} = external power
P_{jet} = jet power
P_{mag} = electromagnetic coil power
P_t = total input power
T = thrust
T_e = electron temperature
T_m = thrust (including multiple charge species)
V_b = beam voltage
V_c = coupling voltage
V_{CG} = cathode-ground voltage
V_d = discharge voltage
V_{PG} = plasma potential-ground voltage
ν_e = electron velocity
α_3 = thrust correction factor (including multiple charge species)
α_m = mass utilization correction factor (including multiple charge species)
$\langle v_b \rangle$ = average ion exit velocity
β = plasma ion current coefficient
γ = thrust correction factor
η_b = current utilization efficiency
η_c = cathode efficiency
η_e = electrical efficiency
η_{ext} = external power efficiency
η_m = mass utilization efficiency
η_v = voltage utilization efficiency
η_t = total thruster efficiency
θ = divergence half angle

I. Introduction

The maturity of electric propulsion (EP) technologies has enabled several science missions to use EP as the main on-board propulsion system and dozens of commercial communications satellites to use EP for station keeping. The two types of electric thrusters that are the most widely used are ion thrusters and Hall thrusters. Both of these technologies offer several system advantages over chemical propulsion systems, chief among them being much higher specific impulse.[1]In the United States, ion thruster research and development was emphasized through the 1990's, and these thrusters were the first to fly on U.S. communications satellites and deep space missions. However, interest in Hall thruster research and development in the United States has increased significantly since the early 1990s. Hall thrusters offer system advantages over ion thrusters, namely the total system cost is lower making the Hall thruster a potentially more desirable option for cost capped missions.[2]To date, over 250 Hall thrusters have been flown in orbit[3] on Russian, European and American spacecraft, and investigations of the basic physics that govern the thruster performance and life continue.

Hall thruster research in the community has largely been concerned with understanding the mechanmism that determine anode efficiency. Anode efficiency is a measure of how well the thruster converts neutral propellant into beam ions and useful thrust. However, cathode efficiency and cathode coupling voltage are two areas of specific interest in the present investigation aimed at understanding other effects that drive the total thruster efficiency. The cathode flow rate tends to be 5-10% of the anode flow rate, and the total efficiency could potentially be raised by several percent by realizing reductions in the cathode flow. As defined here, the cathode coupling voltage is the potential difference from cathode common to the beam plasma potential. This potential drop is related to how easily the electrons are transported from the cathode to the anode. It has been observed that decreasing the cathode flow rate increases the cathode coupling voltage, and further investigation is needed to understand the impact of this change on the overall efficiency.

There have been several studies investigating the effects of cathode coupling in Hall thrusters. These include studies of the effect of mass flow rate[4,5], cathode type[6], and cathode position[4,5,7,8,9]. Tilly, et al.[4] observed increased (larger in magnitude) coupling voltage with decreased mass flow rate. Several studies noted that cathode placement had an effect on cathode coupling voltage.[4,5,7,8,9]. Tilly suggested that a cathode oriented along the thruster axis and placed as close as possible to the outer magnetic pole provides the lowest coupling voltage.[4] Walker also presented experimental data suggesting that the coupling voltage increases in magnitude with increased distance between the cathode and thruster outer diameter; however, he did not observe a decrease in thruster efficiency with cathode placement.[9] A lower coupling voltage causes the voltage utilization efficiency (the effective beam voltage to discharge voltage ratio) to increase, possibly enabling the total thruster efficiency to also be increased. Hofer, et al. suggested that significant performance improvements to Hall thruster efficiency and cathode coupling may be obtained by placing a cathode on the centerline of the thruster between the inner magnetic pole pieces.[7]

In an effort to understand the physics that govern total thruster efficiency, specific attention is paid here to the effects of an internally mounted cathode versus a traditional externally mounted cathode and the affect of the cathode coupling voltage. A laboratory model Hall Thruster was utilized in investigating both cathode flow rate and cathode coupling effects. The cathodes used for these experiments are two lanthanum hexaboride (LaB_6) hollow cathodes[13] developed at JPL. The efficiency analysis used here was developed by Brophy[10], adopted by Kim[11]. We utilize an evolved version of the improved methodology proposed by Hofer[3]. In this study, it will be shown that utilizing the internally mounted cathode increased the total thruster efficiency by 2-3% over the externally mounted cathode; the 6 kW laboratory Hall thruster operates consistently for discharge powers of 3 and 6 kW. It will also be shown that the total thruster efficiency remains constant for the cathode flow fractions investigated (5-9% of the anode flow rate). It was observed that the cathode to ground coupling voltage was increased in magnitude for decreased cathode flow rate while the total mass utilization was increased for decreased cathode flow rate. The total thruster efficiency is calculated and compared using two separate methods: the first is based on the measured thrust while the second is based on external plasma diagnostics to deduce beam current, beam voltage, and species fractions; they agree with 1-3%. The diagnostics used for the two separate methods are discussed in the next section.

II. Experimental Apparatus

A photograph of the 6 kW thruster inside the vacuum chamber is shown Figure 1, where two set of diagnostics, the thruster, and the facility are indicated by numbers. The following sections explain and describe each in detail.

1. Vacuum Facility

The experiments were conducted in the Endurance Test Facility at the Jet Propulsion Laboratory (JPL). The vacuum chamber, which measures 3 m in diameter and 10 m in length, was used for the 30,000 hour Extended Life Test of the NSTAR ion thruster.[12] The vacuum chamber provides a total xenon system pumping speed of approximately 200,000 l/s. The vacuum system provided a background pressure of 1.7×10^{-5} Torr at a xenon flow rate of 22.4 mg/s. At this background pressure, ingestion from background gases are negligible[7] and are not included in the efficiency analysis presented in this paper. The vacuum chamber is lined with graphite panels to reduce the amount of back sputtered material on the thruster and diagnostics.

Commercially available power supplies and flow controllers were used in the operation of the Hall thruster. The propellant flow control system consisted of ¼ inch stainless steel tubes and three mass flow controllers; two 50 sccm controllers, one for each cathode, and one 500 sccm controller for the main anode flow line. Two 500 V-20 A laboratory power supplies connected in either series or parallel powered the main discharge. Four 40 V-19 A laboratory power supplies were used for the inner magnetic coil, outer magnetic coil, internal trim coil, and cathode heater. A 600 V-2.6 A power supply was used for the cathode keeper. The cathode keeper and heater were not used during nominal thruster operation. A data acquisition system was used to monitor the vacuum facility and thruster telemetry. Additional details of the test facility and power electronics can be found in reference 7.

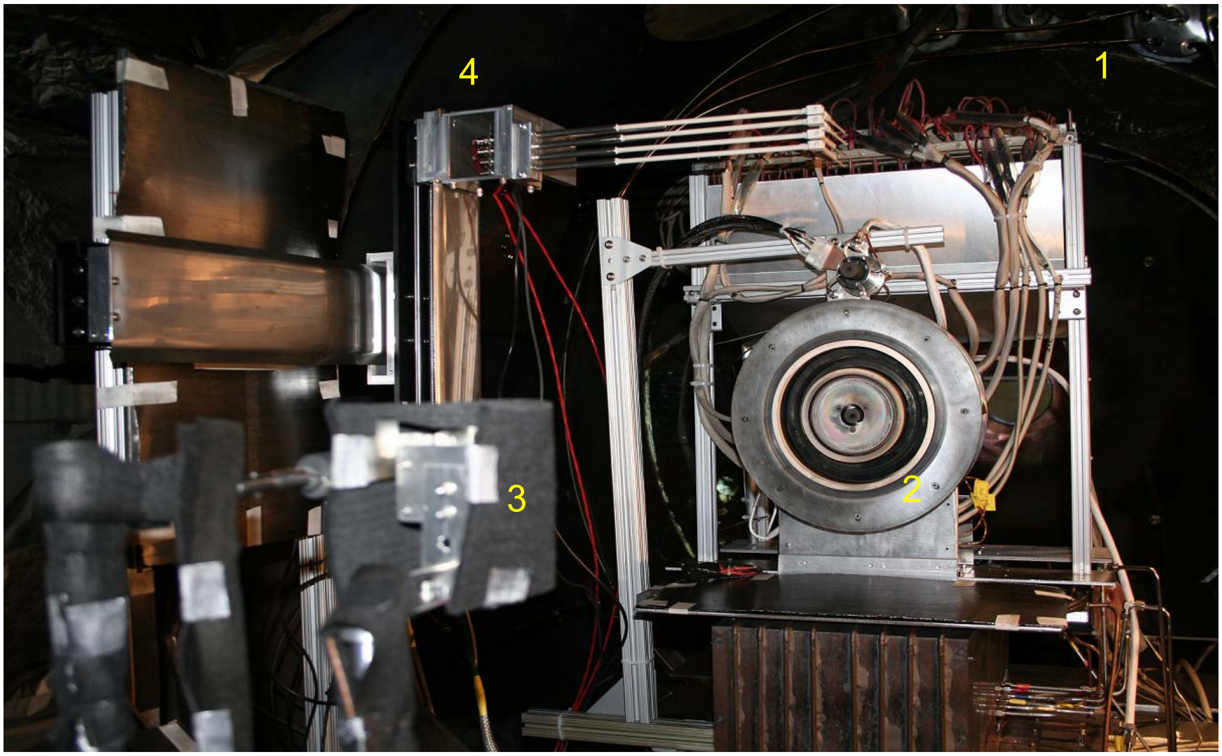

Figure 1. Photograph of the laboratory Hall thruster in the vacuum chamber with various diagnostics; 1, vacuum facility, 2 Hall thruster, 3 far-field probe array, 4 near-field probe array.

2. Hall Thruster and Hollow Cathodes

Figure 2 shows a close up of the 6 kW laboratory model Hall thruster used for these experiments. The nominal power of the thruster is 6 kW, with 300 V, 20 A representing the nominal operating condition. Performance measurements when operating the thruster at the nominal operating condition and with an internal trim coil have shown that the thrust, total specific impulse and total efficiency were 409 mN, 1950 s and 64%, respectively. The thruster is capable of throttling over 2-12 kW discharge power, 1000-3000 s specific impulse, and 100-500 mN thrust. For this specific set of experiments, two power levels were investigated; the designed power level of 6 kW (300 V and 20 A) and a half power level of 3 kW (300V at 10A). Due to the dimensions of this Hall thruster, an internally (or centrally) mounted hollow cathode can be employed. Experiments were conducted with both externally and internally mounted cathodes.

Two Lanthanum Hexaboride (LaB_6) hollow cathodes are also shown in Figure 2; they are labeled as Figure 2a (internal) and Figure 2b (external). Both cathodes were mounted to the thruster at the same time allowing the thruster to be operated with either cathode without breaking vacuum. The LaB_6 hollow cathodes used are configured similar to conventional barium oxide (BaO) dispenser hollow cathodes. However, they

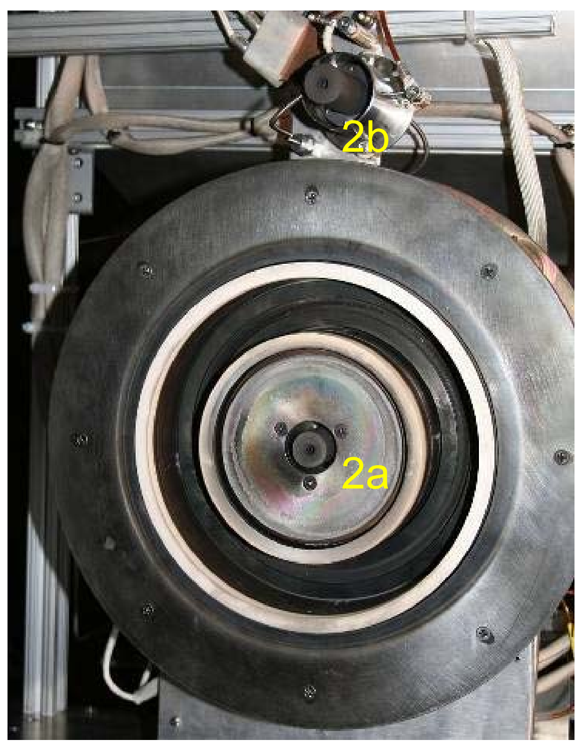

Figure 2. Laboratory Hall thruster with two LaB_6 hollow cathodes; 2a the internally mounted cathode and 2b the externally mounted cathode.

require slightly different material interfaces to the LaB_6 insert. LaB_6 offers advantages over conventional hollow cathodes due to the less stringent xenon purity and handling requirements.[13] The experiments presented here compare thruster performance and efficiency differences for the internal versus external mounted cathodes. No efforts were taken to optimize external cathode position. Tilly and Walker both showed data where the cathode to ground voltage increased in magnitude as the radial distance between the cathode and thruster increased.[4,9] Tilly suggested that an external, axially aligned hollow cathode placed as close to the thruster and outer front pole piece as possible minimizes the cathode to ground floating potential.[4] This suggestion was followed when selecting the external cathode position. The external hollow cathode was axially aligned to allow a direct comparison to the internally mounted cathode. Both cathode keeper orifice exits were flush with the thruster exit plane.

3. Far-Field Probes

Several diagnostics were used to measure the beam characteristics of the thruster. The far-field diagnostics included an ExB probe and an array with a Faraday probe, emissive probe, and retarding potential analyzer (RPA) grouped together. Figure 3 shows the array of far-field probes. However, it does not show the separate ExB probe. When the far-field probes were not in use, they resided behind a graphite-felt lined panel placed close to the chamber wall which protected the sensitive array of diagnostics from ion bombardment. The far-field probe array was attached to a 2-axis probe drive. The axial drive had a range of 43 cm. The radial probe drive had a range of 180 cm and traversed across the thruster exit plane at 6 cm per second.

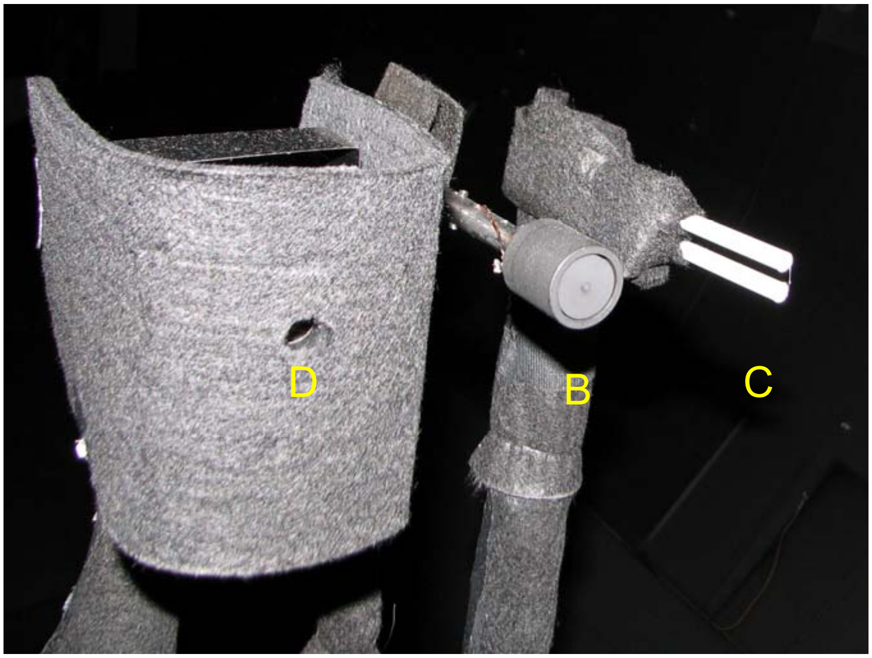

Figure 3. Array of far-field probes, A ExB probe (not shown), B Faraday probe, C emissive probe, and D RPA.

A. ExB Probe

An ExB probe, also known as a Wein filter, was used here to measure the quantity of the different ion species in the beam. An ExB probe discriminates ions according to their velocities through the application of crossed electric and magnetic fields.[7,16,17] From the distribution of measured peaks of ion current, ion species fractions can be computed. The ExB probe used for this experiment was placed approximately 10 thruster outer diameters downstream of the thruster exit plane on the thruster center line. For further specific details on the operation and design of the ExB probe see reference 16. A correction was made for the loss of current supplied by singly-charged xenon ions due to charge-exchange collisions with the neutral background gas.[7] The measurement uncertainty of the ion species fractions was estimated to be ±0.04, ±0.02, and ±0.01, for Xe^{+}, Xe^{++}, and Xe^{+++}, respectively.

B. Faraday Probe

A Faraday probe was used to measure ion current density at approximately 5-7.5 thruster diameters downstream of the thruster exit plane. The Faraday probe consisted of a negatively biased 2 cm outer diameter collection electrode enclosed within a 2.6 cm outer diameter guard ring. The guard ring and collector were fabricated from graphite to minimize probe sputtering from ion bombardment. The collector electrode was biased at -30 V below chamber ground to repel electrons.

C. Emissive Probe

An emissive probe was used to measure the plasma potential in the far-field region of the thruster plume. The emissive probe consisted of a 0.5 mm diameter 26% tungsten-rhenium hair-pin wire 1.75 cm long. The hair-pin wire was fed through two side-by-side 0.635 cm diameter alumina tubes. A floating 10 A power supply provided the current to heat the tungsten wire electrode to emit electrons.

D. Retarding Potential Analyzer

A gridded retarding potential analyzer (RPA) was used to determine the ion energy distribution. A three-grid arrangement was used where the first grid in contact with the plasma was allowed to electrically float, the second grid was biased to repel electrons, and only the ions with energy greater than potential applied to the last discriminator grid could pass through and reach the collector. The RPA was used to measure ion voltage distributions on axis at 7.4 thruster outer diameters downstream of the thruster exit plane.

4. Thrust Stand

The Hall thruster was placed on the same inverted pendulum thrust stand that was employed in the long duration test (LDT) of the NSTAR ion thruster.[12,16] The thrust stand was modified with stiffer springs and heavier weights to accommodate the higher mass of the Hall thruster. The thrust stand deflection was measured with a linear variable differential transducer (LVDT), and was calibrated by the addition of the weights simulating thrust applied to the thrust stand. In order to quantify the long term drift of the thrust stand, periodic calibrations were taken. Uncertainties in the LVDT voltage amounts to ±1% of the total measurement for the thrust stand.

5. Near-field probes

A close up photograph of the near-field probe array consisting of two emissive probes, one ion saturation current probe, and one Langmuir probe is shown in Figure 4. The probes were mounted vertically in the vacuum chamber (see Figure 5). The near-field probes were mounted on a two axis probe drive that had a vertical scan range of 45 cm and had an axial range of 0.75 cm to 21 cm downstream of the thruster exit plane. The probe array was made of four separate L-shaped alumina tubes that housed each of the electric probes. Each probe had an elbow to make the 90^o turn for the correct probe orientation to the thruster plume. The probe tips sat approximately 15 cm upstream of the stabilizing elbow that allowed the plasma to be in an unperturbed state with respect to the large surface area of the alumina tubes and elbows. When the probe array was not in use, it resided in the farthest upstream axial position 15 cm above the thruster outer diameter, also shown in Figure 5.

The Langmuir probe tip was 0.5 mm diameter tungsten wire that was 2.5 mm long. The probe tip protruded out of a 3 mm alumina tube. The bias voltage applied to the probe tips was generated by a programmable waveform synthesizer that drove a 100 V-2 A Kepco bipolar power supply. The voltage waveform was a sawtooth ramp that scanned from –30 to + 90 V in the thruster plume in approximately 2 ms. Several voltage sweeps were taken for each radial scan allowing the Langmuir probe to collect current across the entire thruster exit plane in one sweep. The position uncertainty for the plasma parameters is on the order of 1.5 mm over most of the scan and less than 1 mm near the full insertion point. The probe position, voltage and current data were collected on a computer at a sample rate of 111 kHz, resulting in 1000 data points in each probe characteristic curve. The plasma potential and electron temperatures were computed using classical thin sheath Langmuir probe

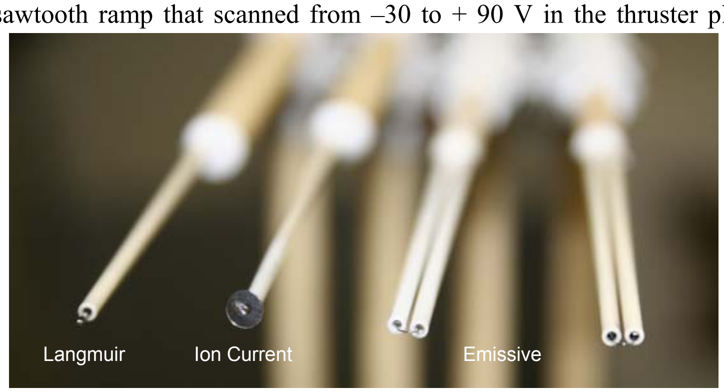

Figure 4. Close up photograph of the near-field probes: Langmuir, ion saturation current, and emissive probe tips.

analysis. The electron temperature is found by fitting an exponential curve to the electron retardation region of the Langmuir trace. The electron temperatures have uncertainties of approximately ±1 V and the plasma potentials have uncertainties of ±3 V.

The ion current probe consisted of a 3.2 mm circular molybdenum disk. The probe was biased at -60 V to collect ion saturation current at axial locations 0.75 cm to 21.0 cm downstream of the exit plane. A flat circular disk probe was chosen to collect beam ions in the channel region of the plume.

The emissive probe was used to determine plasma potential from the thruster exit plane to the near-field region of the thruster plume. The emissive probe consisted of a 0.125 mm diameter tungsten hair-pin wire that was 4 mm in length. The hair-pin wire was fed through two side-by-side 3 mm diameter alumina tubes. Figure 6 shows a close up of an individual emissive probe tip. A floating 5 A power supply provided the current to heat the tungsten wire electrode to emit electrons. Two interchangeable emissive probes were mounted on the near-field probe array to provide a redundant plasma potential diagnostic in the event that one of the probes failed.

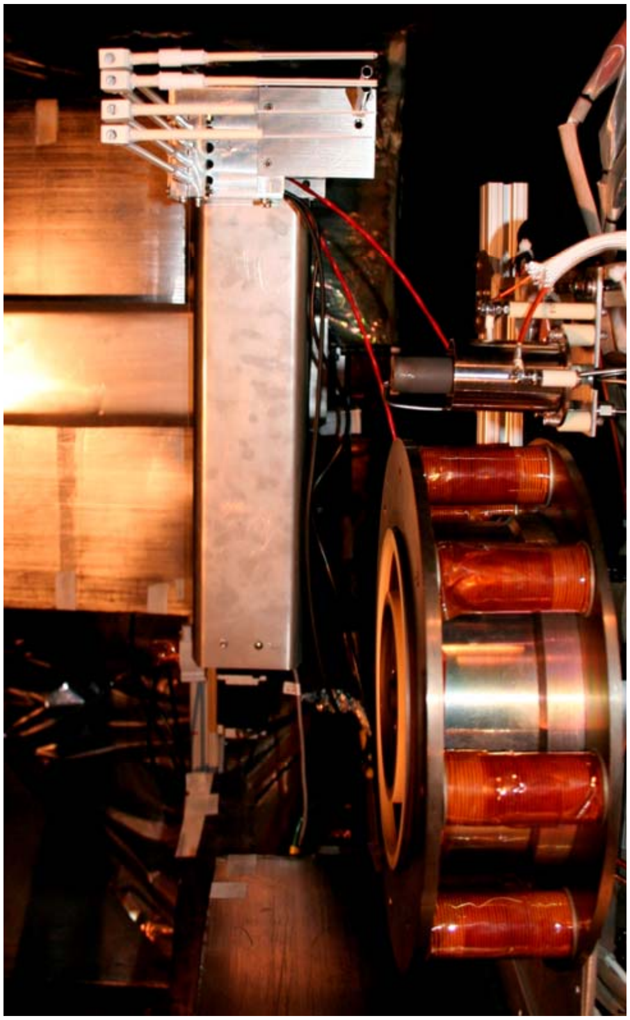

Figure 5. Near-field probe array relative to thruster.

Figure 6. Close up of an emissive probe tip.

III. Results

A. Efficiency Analysis

In order to quantify the effects of changing operating conditions on the Hall thruster, some analysis is needed. Presented below are the equations necessary to calculate the thrust efficiency at each operating condition by two methods. In the first method, thrust efficiency is defined as the ratio of jet power in the exhaust to the total input power given by

$$\eta_t = \frac{P_{jet}}{P_t} = \frac{1}{2}\frac{T^2}{\dot{m}_t P_t}, \quad (1)$$

where T is the thrust, $\dot{m}_t$ is the total mass flow rate, and P_t is the total power needed to operate the Hall thruster including the power to run the magnet supplies. Eq. 1 is the traditional way to calculate total thruster efficiency. This equation will be the baseline efficiency equation, where thrust is measured by a thrust stand.

The second method to calculate total thruster efficiency is based on individual efficiency terms and is similar to the method proposed by Hofer[3] but modified to explicitly account for the effects of plume divergence. Below is a derivation explaining each individual utilization efficiency and total thruster efficiency. In a Hall thruster, propellant is supplied to both the cathode and the anode, and the total mass flow rate is given by

$$\dot{m}_t = \dot{m}_a + \dot{m}_c \, , \tag{2}$$

where $\dot{m}_t$, $\dot{m}_a$, and $\dot{m}_c$ are the total mass flow rate, anode flow rate, and cathode flow rate, respectively. Cathode efficiency is defined as the ratio of anode flow rate to the total flow rate given by

$$\eta_c = \frac{\dot{m}_a}{\dot{m}_t} = \frac{\dot{m}_a}{\dot{m}_a + \dot{m}_c} \, . \tag{3}$$

Mass utilization efficiency characterizes how effective the neutral propellant flux is converted into ion flux and is defined as the ratio of the ion mass flow rate to the total mass flow rate given by

$$\eta_m = \frac{\dot{m}_b}{\dot{m}_t} \, , \tag{4}$$

where the ion mass flow rate is defined as,

$$\dot{m}_b = \frac{I_b M}{e} \, . \tag{5}$$

Mass utilization efficiency is directly related to cathode efficiency and is given as,

$$\eta_m = \frac{\dot{m}_b}{\dot{m}_t} = \frac{I_b M}{e\dot{m}_t} = \frac{\dot{m}_b}{\dot{m}_a}\eta_c \, . \tag{6}$$

Since Hall thrusters produce a significant number of multiply-charged ions, the expression for the mass utilization efficiency must then be modified. For singly, doubly, and triply-charged ions, the corrected mass utilization efficiency is,

$$\eta_m = \alpha_m \frac{I_b M}{e\dot{m}_t} \, , \tag{7}$$

where α_m is defined as[18],

$$\alpha_m = \frac{1 + \frac{1}{2}\frac{I^{++}}{I^{+}} + \frac{1}{3}\frac{I^{+++}}{I^{+}}}{1 + \frac{I^{++}}{I^{+}} + \frac{I^{+++}}{I^{+}}} \, , \tag{8}$$

and I^{++}/I^{+} and I^{+++}/I^{+} are the fractions of double ion current and triple ion current in the beam for the specific operating condition.

Current utilization efficiency characterizes how effectively the electrons are used to ionize the propellant. The current utilization efficiency is defined as the ratio of the ion beam current to the discharge current given by

$$\eta_b = \frac{I_b}{I_d}. \tag{9}$$

Ideally, the ions that are produced in a Hall thruster would be accelerated over a potential drop that is equal to the applied discharge voltage. However, this is never the case. Figure 7 schematically represents the potential distribution in a Hall thruster.

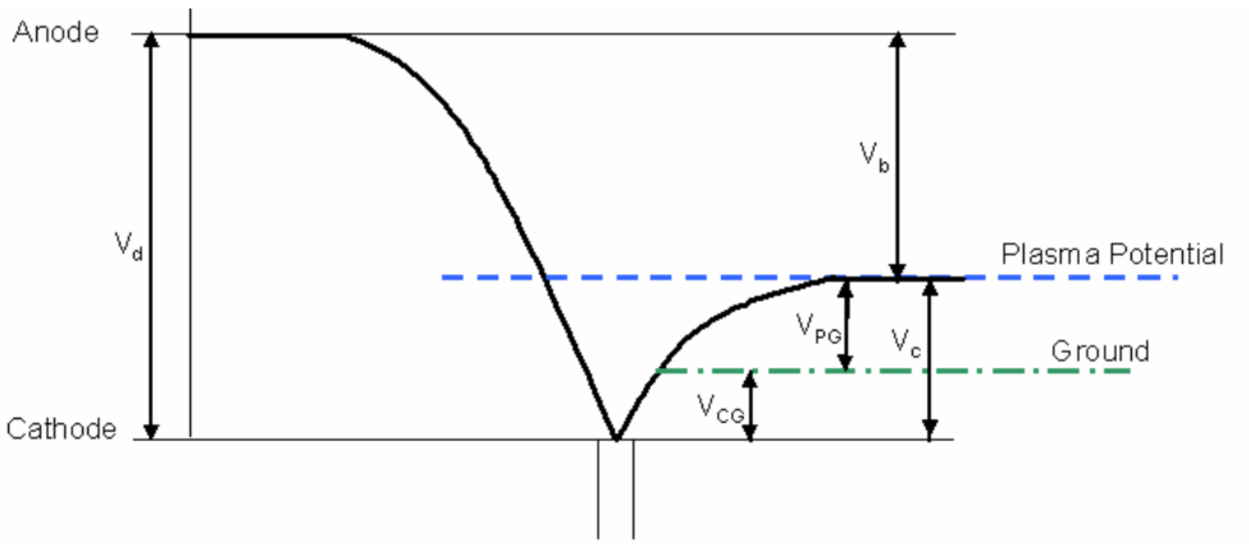

Figure 7. Voltage distribution of a Hall Thruster (not to scale).

The cathode in a Hall thruster typically floats 20 to 40 V below the beam plasma potential. The beam voltage is then defined as

$$V_b = V_d - V_c, \tag{10}$$

where V_c is the coupling voltage. Next, the voltage utilization efficiency (also sometimes called the acceleration efficiency) is defined as the ratio of beam voltage to discharge voltage given by

$$\eta_v = \frac{V_b}{V_d} = \frac{V_d - V_c}{V_d}. \tag{11}$$

The total power input is given by

$$P_t = P_d + P_{mag} + P_{aux}, \tag{12}$$

where P_d is the discharge power ($P_d = V_d \cdot I_d$), P_{mag} is the power to run the magnetic circuit, and P_{aux} is the power to run the any auxiliary units, such as the cathode keeper if used during thruster operation. The magnetic circuit and auxiliary power required to run a Hall thruster can be simplified into one term, the external power, which is defined here as $P_{ext} = P_{mag} + P_{aux}$. The external power efficiency can be defined as the ratio of discharge power to the total input power given by

$$\eta_{ext} = \frac{P_d}{P_t}. \tag{13}$$

Thrust is defined as the sum of all the particle flow rates times their individual velocities. These particles include neutrals, electrons and each ion species (XeII, XeIII, etc.). The ion momentum flux dominates over the electrons and neutral particles because of the large differences in mass and velocity, respectively.[3] Therefore, thrust is defined as

$$T = \sum_{k=1}^{N} \dot{m}_k \langle v_k \rangle , \tag{14}$$

where the index k indicates the charge-state of each ion species, N is the total number of species, and $\dot{m}_k$ and $\langle v_k \rangle$ are the mass flow rate and average velocity of the k^{th} ion species, respectively. Assuming at first only the singly-ionized xenon contributes to the thrust produced, the average exit velocity from conservation of energy is given by

$$eV_b = \frac{1}{2} M \langle v_b \rangle^2 , \tag{15}$$

where V_b is the net voltage through which an ion was accelerated, M is the mass of an ion particle, and $\langle v_b \rangle$ is the average exit velocity of an ion. Rearranging Eq. 15 and solving for the velocity gives

$$\langle v_b \rangle = \sqrt{\frac{2eV_b}{M}} . \tag{16}$$

Thrust for a single species of ions is given by

$$T = \frac{I_b M}{e} \sqrt{\frac{2eV_b}{M}} . \tag{17}$$

For Hall thrusters, corrections are needed to this thrust equation. First, the thrust vector that is produced is never 100% in the same direction, it may have some angular distribution about the normal thrust vector. The correction to the force due to the effective thrust-vector angle is simply

$$F_t = \cos\theta , \tag{18}$$

where θ is the average half-angle divergence of the beam.

A second correction must be made to the thrust equation for the presence of multiple ion species. If the beam contains singly-charged, doubly-charged, and triply-charged ions, the total beam current is

$$I_b = I^{+} + I^{++} + I^{+++} , \tag{19}$$

where I^{+}, I^{++}, I^{+++} is the singly-charged, doubly-charged , and triply-charge ion current, respectively. The total thrust for the multiple species, T_m, is the sum of the thrust from each species:

$$T_m = I^+ \sqrt{\frac{2MV_b}{e}} + I^{++} \sqrt{\frac{MV_b}{e}} + I^{+++} \sqrt{\frac{2MV_b}{3e}} = \sqrt{\frac{2MV_b}{e}} \left(I^+ + \sqrt{\frac{1}{2}} I^{++} + \sqrt{\frac{2}{3}} I^{+++} \right) . \tag{20}$$

The thrust correction factor, α, for thrust in the presence of doubly and triply-ionized atoms is[18]

$$\alpha_3 = \frac{I^+ + \sqrt{\frac{1}{2}} I^{++} + \sqrt{\frac{2}{3}} I^{+++}}{I^+ + I^{++} + I^{+++}} = \frac{1 + 0.707 \frac{I^{++}}{I^+} + 0.816 \frac{I^{+++}}{I^+}}{1 + \frac{I^{++}}{I^+} + \frac{I^{+++}}{I^+}} , \tag{21}$$

where I^{++}/I^+ and I^{+++}/I^+ are the fractions of double and triple ion current in the beam. The total thrust including triples is given by

$$T = \alpha_3 F_t \sqrt{\frac{2M}{e}} I_b \sqrt{V_b} . \tag{22}$$

The correction for both of these effects can be combined into the total thrust correction factor γ, and is defined as

$$\gamma = \alpha_3 F_t . \tag{23}$$

Using the definition of total thruster efficiency defined in Eq. 1 and substituting in Eq. 7, 9, 11, and 13 the total thrust efficiency can be written as a function of the individual utilization efficiency terms given by

$$\eta_t = \frac{1}{2} \frac{T^2}{\dot{m}_t P_t} = \frac{1}{2} \frac{T^2}{\dot{m}_a P_d} \eta_c \eta_{ext} = \gamma^2 \frac{I_d M}{e} \frac{1}{\dot{m}_t} \eta_b \eta_v \eta_{ext} , \tag{24}$$

$$\eta_t = \gamma^2 \frac{I_d M}{e} \frac{\eta_c}{\dot{m}_a} \eta_b \eta_v \eta_{ext} , \tag{25}$$

$$\eta_t = \gamma^2 \eta_m \eta_b \eta_v \eta_{ext} . \tag{26}$$

The individual thruster efficiency terms are evaluated using the plasma diagnostics described in the Experimental Apparatus section. The results of calculating total thruster efficiency using Eq, 1 and Eq. 26 are presented below.

B. Far-field Probe Results

Far-field probes were used to measure plasma parameters that aid in calculating the individual thruster efficiency terms given in Eq. 7, 9, 11, 13 and the thrust correction factor given in Eq. 26. The ExB probe was used to calculate the species fractions present in the plume. The ExB probe was placed on the centerline of the thruster plume 10 thruster outer diameters downstream of the thruster exit plane. A single-point measurement was used in estimating the far-field species fractions present in this thruster plume. A typical ExB trace is shown in Figure 8. There are three distinct regions in the trace; the largest peak corresponds to the collected single ion current, the next largest peak corresponds to the double ion current and so on and so forth. For all ExB traces and analysis, any ion charge state higher than a triply-charged ion was neglected. The single ion current was also corrected for the presence of charge exchange with the neutral back ground gas in the vacuum chamber. For this particular trace at the 6 kW internal cathode condition, the calculated doubles to the total species fraction is 7.2% and the triples to the total species fraction is 1.7%.

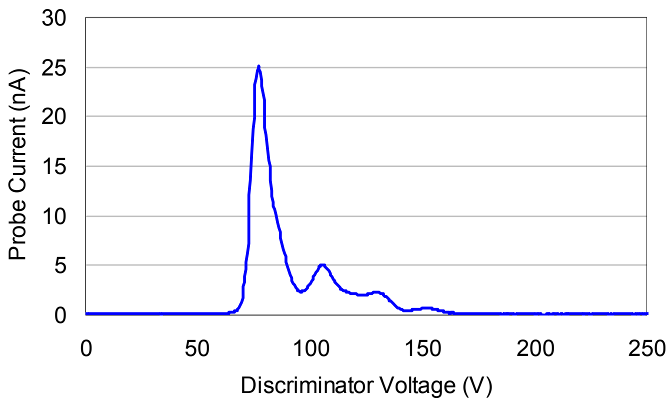

Figure 8. A typical ExB probe trace at 6 kW for the internal cathode.

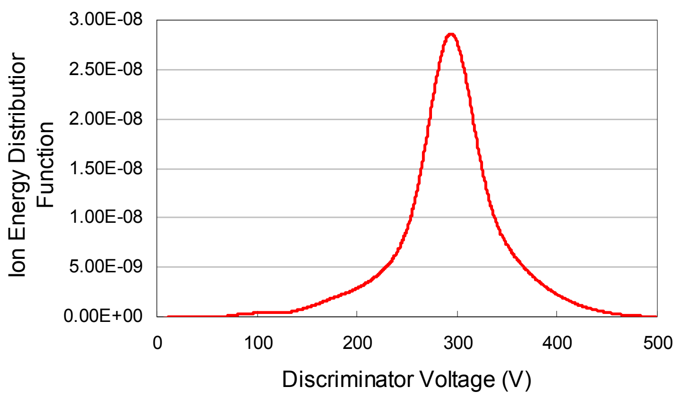

Figure 9. A typical RPA trace at 6 kW for the internal cathode.

The emissive probe technique is a way to measure the plasma potential directly without any further analysis such as finding the plasma potential using a Langmuir probe trace. All plasma potentials used in the efficiency analysis were measured directly from the far-field or near-field emissive probes. The plasma potentials in the far-field were measured on the thruster centerline 7.4 thruster outer diameters downstream of the exit plane. For the 6 kW internal cathode position the plasma potential was 11 V.

The beam voltage V_b, the voltage through which ions are accelerated, can be deduced from knowing the beam plasma potential and the average ion energy given by a RPA trace. The derivative of an RPA trace yields the ion energy distribution for the beam. Figure 9 shows a typical first derivative of the RPA trace for the 6 kW internal cathode condition. This trace was taken on the thruster centerline 7.4 thruster outer diameters downstream of the exit plane. The RPA provides the ion energy distribution with respect to chamber ground. As seen in Figure 7, to calculate the beam voltage, the plasma potential must be subtracted from the peak voltage from the distribution. For the 6 kW internal cathode condition the beam voltage was 281 V. The applied voltage between the anode and cathode is 300 V for this condition, which gives a voltage utilization efficiency of 93.7%.

C. Near-field Probe Results

The ion current probe in the near-field probe array was used to calculate the ion beam current. For the efficiency analysis presented here, ion current was calculated from the radial trace taken 0.75 cm downstream of the thruster exit plane. Figure 10 compares radial profiles of ion current density for the internal and external cathodes. The internal cathode produces a large spike in the ion current density on the centerline of the thruster, which can be seen in Figure 10a. In order to calculate the beam current, this spike was neglected because the ions from the cathode are slow and do not contribute to beam current. The ion current was then calculated by integrating the area under the curve over the channel area. The current utilization efficiency was calculated by dividing the beam current by the discharge current. The 6 kW internal cathode condition yields a beam current of 15.63 A, producing a current utilization efficiency of 78.0%. The same approach of neglecting the ion current contribution from in front of the cathode was also used when calculating the beam current for the external cathode. The 6 kW external cathode condition yields a beam current of 15.31 A, producing a current utilization efficiency of 76.7%.

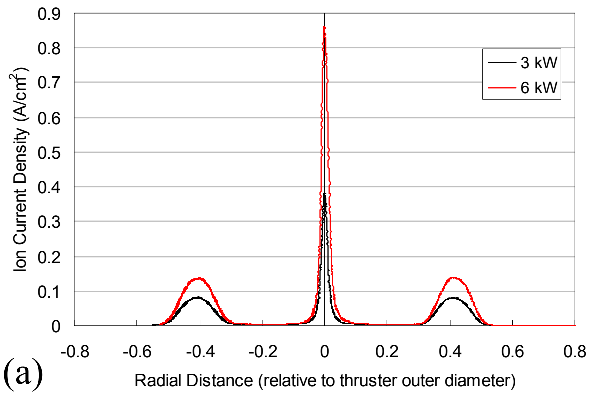

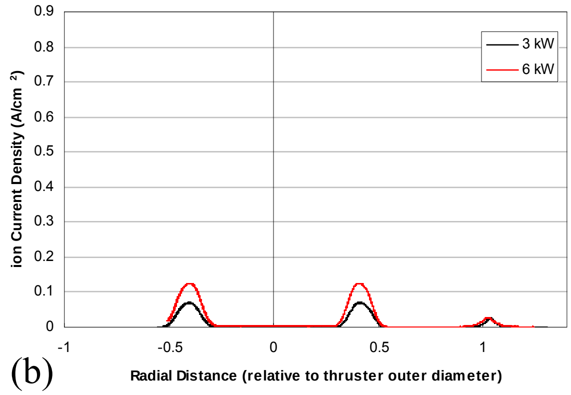

(a) (b)

Figure 10. Ion Saturation Profiles at an axial location 0.75 cm downstream of the thruster exit plane for (a), the internal cathode and (b) the external cathode.

Comparing the graphs in Figure 10, the differences in the beam current for the internal and external cathodes for the 6 kW power condition seem negligible. Figure 11 is a blow up of the ion current density collected over the discharge channel for both internal and external cathodes at 6 kW. This figure shows in more detail that the probe collects higher current for the internal cathode condition over the same area compared to the external cathode case, leading to the 1.3% increase in current utilization efficiency.

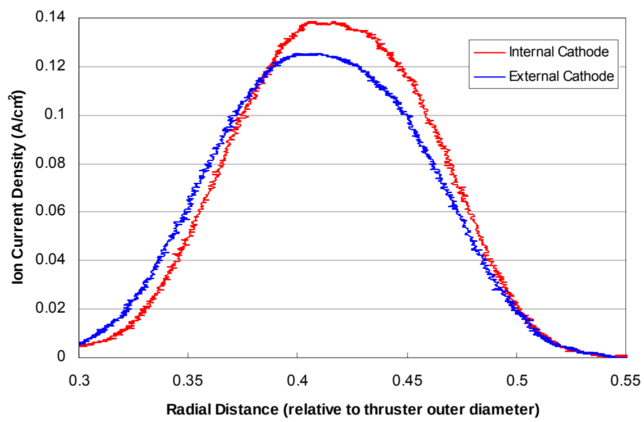

Figure 11. Close up comparison of ion current density profiles at the 6 kW condition over the discharge channel width.

Figure 12 shows a comparison of the ion saturation current density for the 3 kW internal cathode condition for radial scans taken at 0.75 cm and 21 cm downstream of the thruster exit plane. Integrating the radial trace taken at 0.75 cm over the channel width gives a beam current of 8.70 A, while integrating the radial trace at 21 cm over the outer thruster diameter gives a beam current of 8.92 A. The 2.5% difference in ion current density from the radial scans taken at 0.75 cm to 21 cm suggests that the planar ion saturation probe is a good design for collecting beam ions in the range of the thruster exit plane to the near-field. In Hall thrusters the beam will eventually cross over at some point downstream. At 21 cm downstream of the thruster exit plane, the radial scan of the plume is more likely to not be symmetric due to this cross over, where the radial scan at 0.75 cm downstream of the thruster is very symmetric, as seen in Figure 10. Due to the symmetry in the radial traces at 0.75 cm, this location was chosen to calculate beam current.

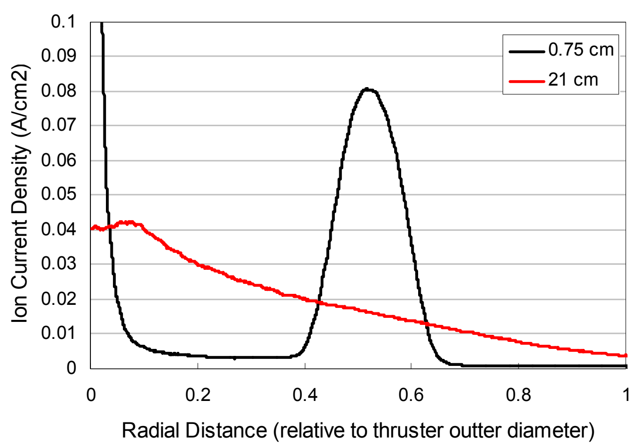

Figure 12. Comparison of ion current density profiles for the 3 kW condition at two axial locations, 0.75 cm and 21.0 cm downstream of the thruster exit plane.

In addition, the axial location of 0.75 cm was chosen for the calculation of beam current because it is likely that the majority of the ionization and acceleration occurs upstream

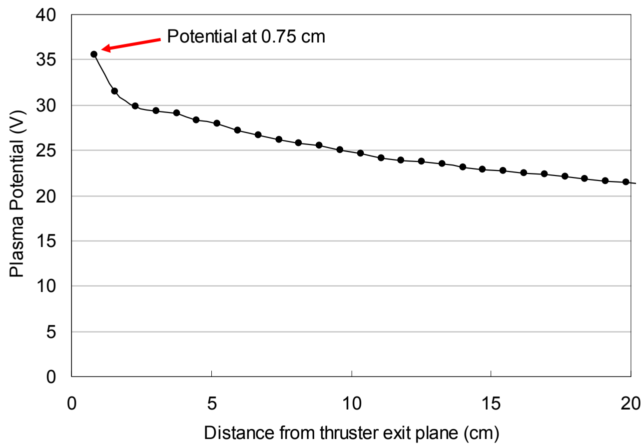

Figure 13. Axial plasma potential profile on the channel centerline for the 6 kW internal cathode position.

of this location and the planer probe will collect nearly all the ion current produced in the discharge channel. Figure 13 shows axial data of the plasma potential on the channel centerline from 0.75 cm to 21 cm downstream of the thruster exit plane. Any ionization downstream of the 0.75 cm axial location will result in ions that gain very little energy (≈15 V) and so will not significantly contribute to the thrust.

Plasma potential measurements in the thruster plume are required to calculate the effective beam voltage. Radial plasma potential traces at 21.0 cm downstream of the thruster exit plane are shown in Figure 14 for both the internal and external cathodes at the 3 kW and 6kW power levels. To calculate the beam voltage, the same method was employed as the far-field probe technique described above. For the 6 kW internal cathode condition the most probable voltage from the RPA trace was shown in Figure 9 and given as 298 V. The plasma potential found from the near-field emissive probe on the center line for the same power level and cathode condition is 19 V. Therefore, the beam voltage equals 278V. The applied voltage between the anode and cathode is 300 V for this condition, which gives a voltage utilization efficiency of 92.6%.

The plasma potential for the internal cathode at 21.0 cm downstream is on the order of 19 V for both power levels, where the plasma potential for the external cathode is on the order of 28 V. The difference in the plasma potential for the two cathode conditions translates into a 4% decrease in the voltage utilization efficiency for the external cathode condition compared to the internal cathode condition.

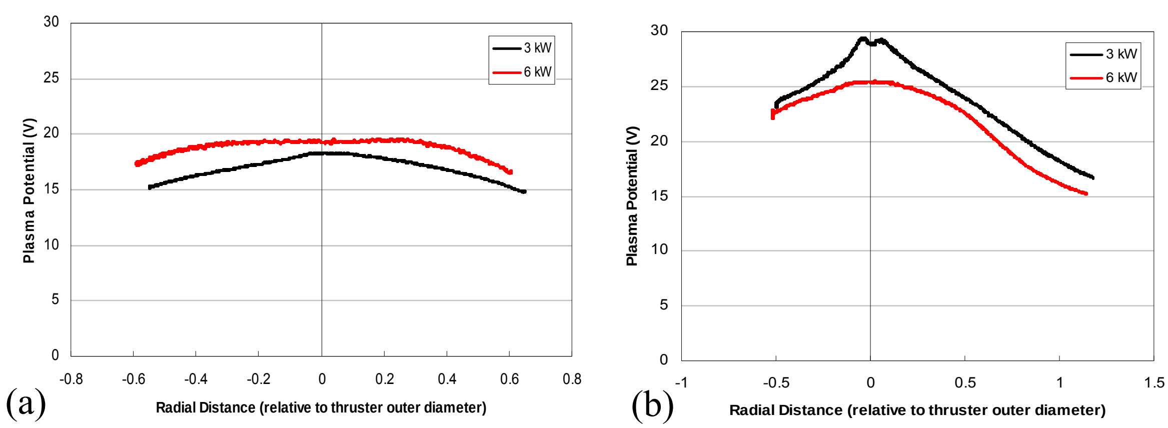

Figure 14. Plasma potential profiles 21.0 cm downstream of the thruster exit plane for (a), the internal cathode and (b) the external cathode.

IV. Discussion

Table 1 is a summary of the individual efficiency terms and total thrust efficiency given by Eq. 1 and Eq. 26 for the internal cathode versus the external cathode at both power conditions. Given in the subsequent paragraphs are more detailed discussions of the individual efficiency terms and total thrust efficiency.

In the Hall thruster, the discharge voltage is controlled and set by the power supply and the discharge current is proportional to the anode mass flow rate. For an applied voltage of 300 V and an anode mass flow rate of 21 mg/s the nominal discharge power is approximately 6 kW. For the same discharge voltage and mass flow conditions, the external cathode does not produce the same amount of discharge power or thrust. Although the difference in discharge power is only 32 W, this suggests the internal cathode is more efficient in generating the beam than the external cathode. A further look into mass, voltage, and current utilization efficiencies shows the same trend in that the internal cathode geometry is more efficient in all these terms and total thrust efficiency.

Table 1. Overview of Hall thruster efficiencies for the internal and external cathode conditions for two power levels, 3 kW and 6 kW.

	"3 kW"		"6 kW"	
	INTERNAL	EXTERNAL	INTERNAL	EXTERNAL
I_d (A)	9.5	9.4	20	19.9
V_d (V)	300.0	300.2	300.3	300.2
P_d (W)	2862	2833	6021	5989
V_{cg} (V)	-11.9	-21.9	-10.76	-16.79
V_c (V)	35.6	46.8	19.6	28.9
I_b (A)	8.7	8.3	15.63	15.31
V_b (V)	264	253	281	271
$\dot{m}_a$ (mg/s)	10.48	10.48	20.96	20.96
$\dot{m}_c$ (mg/s)	0.81	0.81	1.48	1.48
n^{++}/n^{+} species ratio	0.061	0.053	0.070	0.079
n^{+++}/n^{+} species ratio	0.016	0.012	0.022	0.019
γ^2 (assumed 20 degree half angle at 6 kW) (assumed 25 degree half angle at 3 kW)	0.790	0.795	0.844	0.841
$T_{measured}$ (mN)	201.3	195.3	391.7	383.5
$T_{calculated}$ (mN)	208.1	194.9	401.8	382.7
η_m	0.931	0.893	0.912	0.890
η_b	0.912	0.879	0.780	0.767
η_v	0.881	0.844	0.935	0.894
η_{ext}	0.993	0.994	0.995	0.996
η_t (Eq. 26 product of individual efficiencies)	0.587	0.523	0.558	0.517
η_t (Eq. 1 function of measured Thrust)	0.573	0.544	0.565	0.545

Cathode efficiency is the ratio of anode to total flow rate and is an indication of how effectively the cathode is being utilized based on flow rate. Often the cathode efficiency is neglected in performance and efficiency analysis. Mass utilization efficiency is normally defined as the ratio of the mass flow rate of beam ions to the mass flow rate of the anode, where cathode flow is neglected. Keep in mind that this investigation is concerned with the affects of cathode position and cathode flow on total thruster efficiency. Therefore, when calculating the mass utilization efficiency, it is a function of the total mass flow rate and cathode efficiency, as seen in Eq. 6. For the purposes of comparison the cases reported in Table 1 have a cathode flow split equal to 7% of the anode rate, leading to cathode efficiencies of 93.4% for each of the operating conditions. The effects of cathode flow splits will be investigated in subsequent paragraphs.

Mass utilization efficiency is a measure of how effectively the thruster is in taking the neutral propellant and ionizing it, thus turning it into useful ion beam current. The mass utilization efficiency is then calculated by computing the ion mass flow rate divided by the total mass flow rate. The ion mass flow rate is calculated using Eq. 5, where I_b is determined by integrating the ion saturation probe current over the effective area, as shown in Figure 10. The mass utilization efficiencies for the 6 kW condition are both very high: 91.2% for the internal cathode and 89.0% for the external cathode. This suggests that the external cathode configuration does not use the neutral propellant as efficiently as the internal cathode. The mass utilization efficiencies for the 3 kW condition are also both very high: 93.1% for the internal cathode and 89.3% for the external cathode.

Current utilization efficiency characterizes how much of the discharge current in the thruster is carried by beam ions. The current utilization efficiency is calculated by dividing calculated beam current by the discharge current. For the 6 kW condition the current utilization efficiency is 78.0% for the internal cathode and 76.7% for the external cathode. For the 3 kW condition the current utilization efficiency is much larger at 91.2% for the internal cathode and 87.9% for the external cathode. Measurements using gridded Faraday probes to calculate beam current in the far-field of an identical thruster operating at the Air Force Research Laboratory and the University of Michigan have shown similar current utilization efficiencies between 85-90% operating the thruster at the same discharge voltage and an anode mass flow rate of 20 mg/s.[19,20] The higher current utilization efficiency for the 3 kW condition suggests that the current is carried largely by beam ions and the electron current contribution to the discharge is small. For the 6 kW condition where the mass utilization is still high (on the same order as the 3 kW condition for both cathodes), the current contribution from electrons is much larger causing the decrease in current utilization efficiency.

The voltage utilization efficiency is a measure of how much energy the beam ions have compared to the applied discharge voltage. For the internal cathode condition at 6 kW the voltage utilization efficiency is 93.5% while the external cathode condition is 89.4% efficient. The 4% increase in voltage utilization for the internal cathode over the external cathode signifies that most of the internal cathode's beam ions are born at a higher potential than that of the external cathode condition. The effective beam voltage, from Eq. 10, is the difference between the applied discharge voltage and the coupling voltage. The cathode to ground voltage is a direct measurement, and is sometimes reported incorrectly as the coupling voltage. The entire loss voltage (or coupling voltage) is the sum of the measured cathode to ground voltage and the beam plasma potential. Although this is a seemingly straight forward calculation, the plasma potential presents a measurement difficulty. In addition, there is a distribution of energy across the thruster plume as seen in Figure 14. For the efficiency analysis presented in this paper, voltage utilization efficiencies are calculated using plasma potentials on the centerline. Another difficulty is where to physically take the emissive probe data; if taken too far downstream, the measured plasma potential will be unphysically low and will give a falsely high voltage utilization efficiency. It was decided that the plasma potential would be taken at 3 thruster outer diameters, a place where the ions are certainly no longer being accelerated.[21] The plasma potential was taken at 1 and 7.4 thruster diameters downstream, and the plasma potential was interpolated to 3 thruster diameters and used in calculating the voltage utilization efficiency. The 6 kW internal cathode condition and external cathode have a total coupling voltage of 19.6 V and 28.9 V, respectively, leading to voltage utilization efficiencies of 93.5% and 89.4%, respectively. The 3 kW internal cathode and external cathode condition have a total coupling voltage of 35.6 V and 46.8 V, respectively, leading to voltage utilization efficiencies of 88.1% and 84.4%, respectively. The difference in voltage utilization efficiency between the internal cathode and external cathode conditions are approximately 4% for both power levels. This suggests that the internal cathode provides a mechanism for the ions to be accelerated to a higher potential over the external cathode. The 3 kW condition is less efficient overall in accelerating its ions for the applied discharge voltage compared to the 6 kW condition.

Figure 15shows two photographs of the thruster running at 6 kW for the internal and external cathode. In Figure 15b the cathode plume is very visible and has a distinct plume that is pink in color. This pink color is normally indicative of excited neutrals.[22] It can be seen that the electrons are following magnetic field lines that have a return path radially away and perhaps behind the thruster. It is possible that the electric and magnetic field structure in the external cathode case makes it more difficult for electrons to be transported into the thruster channel and contribute to ionization of the neutral propellant.[23] Also the pink cathode plume in Figure 15b shows that some fraction of the electrons emitted by the cathode are expending their energy exciting neutrals. Therefore, the plume shape and color suggest that the external cathode coupling is less efficient than the internal cathode, which is born out by the experimental data.

The total thrust efficiencies calculated from the thrust measurements in Eq. 1 are 56.5% for the internal cathode condition and 54.5% for the external cathode condition at the 6 kW power level. The doubles to singles species ratio and the triples to singles species ratio are given in Table 1. For the 6 kW condition the internal cathode and external cathode the percentages are very similar. Therefore, the calculated α in Eq. 21 does not account for the difference in the total thruster efficiency between the internal and external cathode conditions. The total efficiency calculated from the individual efficiency terms in Eq. 26 are 55.8% for the internal cathode and 51.7% for the external cathode configuration. It was concluded that a divergence half angle of 20^{o} was appropriate for the 6 kW power condition to rationalize the efficiency calculated from Eq. 1 with the efficiency calculated in Eq. 26. For the internal cathode condition, the two efficiencies agree with in about one percent at 6 kW.

In calculating the total thrust efficiency for the 3 kW conditions, the divergence half angle needed to be increased from 20^{o} to 25^{o} in order to match the calculated efficiency from Eq. 26 to Eq. 1. This is consistent with data given by Hofer[3]et al. that showed when the anode flow rate changed from 5 to 15 mg/s for a constant discharge voltage, the divergence half angle decreased about 4-5 degrees. Due to the smaller anode flow rate accompanied to the 3 kW power condition and with a strong magnetic field lens geometry utilized in this thruster, the ions are produced further downstream in the discharge channel than in the 6 kW condition, this causes the beam to be more divergent . The total thrust efficiency calculated from the thrust measurements in Eq. 1 are 57.3% for the internal cathode condition and 54.4% for the external cathode condition at the 3 kW power level. The efficiencies for the 3 kW are on the same order as the 6 kW power level, showing that the thruster operates consistently for the internal and external cathode configurations at both power levels. The total efficiency calculated from the individual efficiency terms in Eq. 26 are 58.7% for the internal cathode and 52.3% for the external cathode for the 3 kW power level.

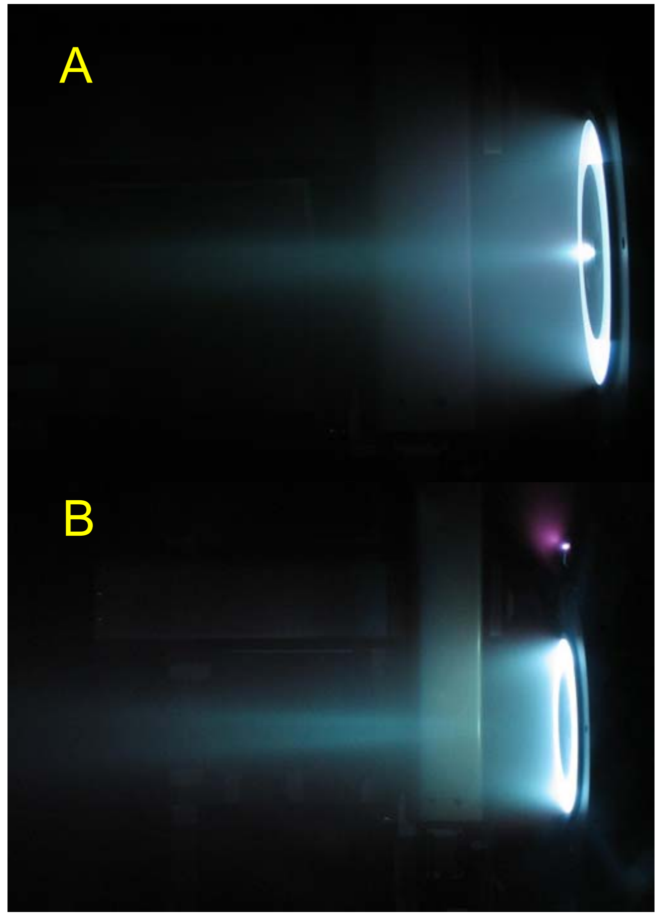

Figure 15. Hall thruster running at 6 kW for (a) internal cathode and (b) external cathode.

Comparing the total thruster efficiencies calculated from thrust and the individual efficiency terms gives insight into which term(s) drives the thruster efficiency in Eq. 26. The traditional way of calculating efficiency using Eq. 1 was utilized as baseline for the thruster efficiency, and has an error determined primarily by the thrust measurement from the thrust stand. Calculating each individual efficiency term in Eq. 26 allows one to dissect the total efficiency and understand how each term contributes to the overall efficiency. However, finding the individual efficiency terms requires 5 separate probe techniques and each one is subject to some error. Yet the difference between the total thruster efficiencies from our measurements is only 1-3% for either cathode condition at both power levels. This small percentage difference gives some confidence that using the probes to measure the necessary quantities and to calculate the individual efficiency terms is a reasonably valid method for determining the total thruster efficiency.

The divergence half angle and the beam current are two quantities to which the total thrust efficiency is most sensitive. The beam current calculation is sensitive to the area over which the integration is performed and as the measurement is made farther down stream where the beam diverges, more uncertainty is introduced into the measurement. Very little if any divergence is seen at the radial trace taken at 0.75 cm, providing another reason the beam current is calculated at this axial location. Choosing divergence half angles of 20^{o} and 25^{o} for the 6 kW and 3 kW power levels allowed the total thruster efficiencies to match within the 1-3% range. The divergence half angle could have been selected such that the two total efficiency terms match within 0.5% for each case, however, the 20° and 25° are representative values chosen from previous published data.[3] Further investigation is needed to understand the dependency of the divergence half angle on total thruster efficiency for the power levels investigated.

Thrust is derived in Eq. 22, and is a direct function of the beam current, the divergence half angle, the thrust correction factor, and the square root of beam voltage. Of the measured quantities (α, I_b, and V_b) the beam current is the most critical factor in calculating thrust. The beam currents measured from the ion saturations probe for the internal and external cathodes at both power levels are given in Table 1. The internal cathode, for both power conditions, yields a higher beam current compared to the external cathode. For a constant beam divergence angle for the internal and external cathode, the higher beam current for the internal cathode suggests that the internal cathode should yield higher thrust than that of the external cathode. This is confirmed by the measured thrust, 391.7 mN for the internal cathode and 383.5 mN for the external cathode for the 6 kW condition, and 201.3 mN for the internal cathode and 195.3 mN for the external cathode for the 3 kW condition.

The source of the improvement in the thruster efficiency for the internal cathode compared to the external cathode can be explained from the individual efficiencies listed in Table 1. We see that the thrust correction factor (γ) and the external efficiency (η_{ext}) are about the same for the two cases. However, all of the other efficiencies for the beam utilization, mass utilization, and voltage utilization efficiencies (η_b, η_m, and η_v) are higher for the internal cathode configuration. This suggests that positioning the cathode on axis results in a plasma structure that turns more of the propellant into useful beam ions, and those ions tend to have higher energy. This is likely caused by an increase in the ionization in the channel upstream of the accelerating potential gradient. Investigations are underway now to understand why the internal cathode location produces this apparently advantageous change in the plasma structure in the channel.

As a part of this investigation, we also examined the impact of cathode flow rate on thruster efficiency. Figure 16 is a plot of the cathode to ground voltage versus the percentage of cathode flow rate. As the cathode flow increases, the cathode to ground voltage decreases in magnitude. This trend was also shown by Tilly[4], however, he did not report a change in total thruster efficiency. Walker[9] investigated thruster performance as a function of cathode position and observed that the cathode to ground voltage increased in magnitude with increased radial distance from the thruster. However, in his investigation he reported that the total thrust efficiency was constant over the radial distance domain.[9] The results presented here show that the total thrust efficiency is independent of V_{cg} within the experimental error of the thrust measurement. Figure 17a shows the measured thrust and Figure 17b shows calculated total efficiency versus percent cathode flow rate for a constant 6 kW of power and 21 mg/s of anode flow rate. The thrust levels shown in Figure 17a are essentially constant with cathode flow fraction. The difference in measured thrust is within the error of the thrust stand over this cathode flow range. The calculated efficiency shown in Figure 17b, therefore, is also constant for the different cathode flow splits. The thrust levels shown in Figure 17a increase slightly with increased cathode flow fraction. However, the calculated efficiency shown in Figure 17b is essentially constant over the measured cathode flow splits. This shows that, even though the coupling to ground increases in magnitude for decrease cathode flow, the thruster efficiency is only weakly affected.

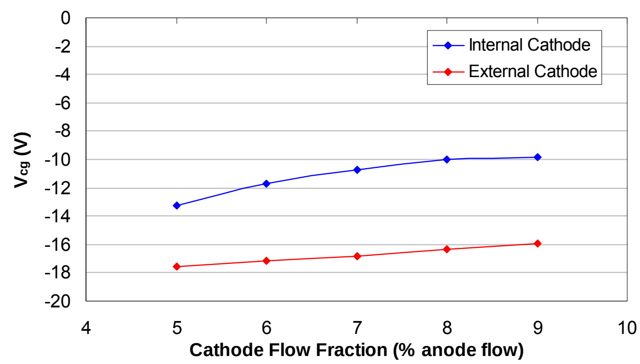

Figure 16. Cathode-common to ground voltage as function of cathode flow rate.

To explain why total thruster efficiency remains constant over the investigated range of cathode flow fractions, the individual efficiency terms from the probe data can be examined. The external power utilization efficiency (η_{ext}), total thruster correction factor (γ), and current utilization efficiency (η_b) remain relatively constant as the cathode flow split changes, and so do not contribute to any changes in the total thruster efficiency. The voltage utilization efficiency (η_v) is found to increase as the cathode flow fraction is increased, corresponding to the decreased cathode to ground coupling voltage. This increase in voltage utilization efficiency in this case is expected from Figure 7as the magnitude of the coupling voltage decreases. However, the mass utilization efficiency (η_m) is found to decrease as the cathode flow split increases. The added cathode flow is not utilized to make thrust ions because it is injected external to the thruster channel. Therefore, the thruster is not turning the added flow through the cathode into useful beam ions, and the mass utilization efficiency decreases. The decrease in mass utilization efficiency off sets the increase in voltage utilization efficiency for increased cathode flow fractions. Therefore, the total thruster efficiency remains constant.

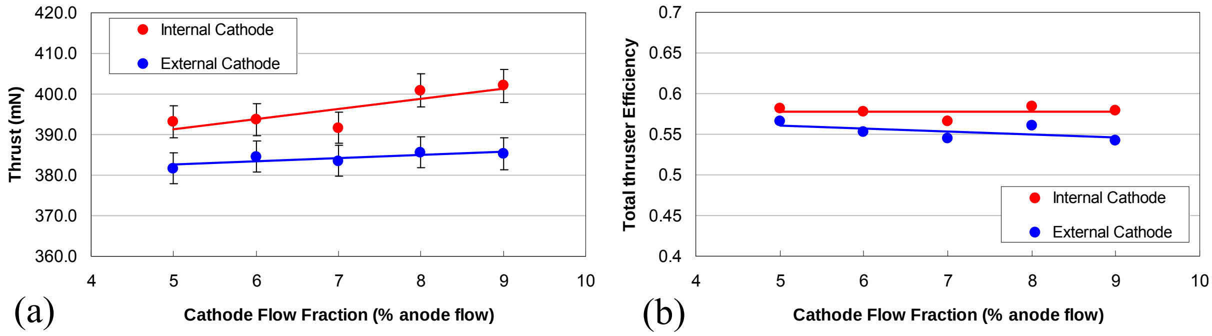

Figure 17. (Figure 17a) Thrust as function of cathode flow fraction (with respect to anode flow rate) and (Figure 17b) Thrust efficiency as function of cathode flow fraction (with respect to anode flow rate), for constant anode flow rate of 21 mg/s and 300 V discharge voltage.

Historical efforts to minimize the directly measured cathode-to-ground voltage (V_{cg}) appear to be unnecessary. Walker presented data where the cathode to ground voltage increased due to cathode placement changes, but the thruster efficiency remained constant.[9] The data shown here in Figure 16 and Figure 17 also has the same trend, where the increased cathode to ground coupling voltage due to changes in flow split does not affect the total thruster efficiency. Research by Goebel[18] and Mikellides[24] suggests that cathode life is extended at lower cathode flow rates than normally used in Hall thrusters. At lower flow rates, more of the cathode's insert is utilized, allowing the cathode insert to operate at a lower temperature, which will increase the life.[18,24] Operating at a lower cathode flow rates also slightly decreases the total amount of propellant needed to run the thruster. Cathode keeper erosion in this case may be of concern, but has been extensively investigated for ion thrusters and Hall thrusters. Mikellides[25]has shown simulations of a hollow cathode with similar dimensions and flow rates (on the order of the 5% flow split, which is approximately 1.06 mg/s or 10 sccm for the 6 kW power condition) in which the cathode keeper was not significantly eroded. Therefore, lower cathode flow splits may be advantageous as longer cathode life is desired for deep space missions since it does not cause a decrease in the thruster efficiency.

V. Conclusion

The effect on total thruster efficiency of an internally and externally mounted cathode, power level, and cathode flow fraction were examined for a laboratory model 6 kW Hall thruster. Data showed that the total thruster efficiency was increased by 2-3% by operating the thruster with the internally mounted cathode versus the externally mounted cathode while the thruster performed similarly at the two power levels investigated (3 and 6 kW). The total thrust efficiency was calculated by two methods; the traditional method based on measured thrust and the second method of using an array of near- and far-field probe diagnostics to calculate individual efficiency terms. The diagnostics included a thrust stand, far-field probes (emissive, Faraday, ExB, and RPA), near-field probes (Langmuir and emissive), calibrated mass flow rate meters, and calibrated voltage and current measurements. The second method produced total thrust efficiencies within 1-3% of the first method, validating the use of the second method for explaining the efficiency behavior of the thruster. In addition, the cathode to ground coupling voltage was observed to increase in magnitude with decreasing cathode flow rate at a constant power level, but the total thruster efficiency was not affected.

Acknowledgments

The research described in this paper was carried out by the Jet Propulsion Laboratory, California Institute of Technology, under a contract with the National Aeronautics and Space Administration.

References

[1]Suttan, G.P. and Biblarz, O., *Rocket Propulsion Elements*, 7th ed., New York, John Wiley& Sons, 2001.

[2]Hofer, R. R., Randolph, T. M., Oh, D. Y., Snyder J. S., "Evaluation of a 4.5 kW Commercial Hall Thruster System for NASA Science Missions," AIAA-2006-4469, 42nd Joint Propulsion Conference, Sacramento, CA, July 9-12, 2006.

[3]Hofer, R. R., "Development and characterization of high-efficiency, high-specific impulse xenon Hall thrusters," dissertation, University of Michigan, 2004.

[4]D. l. Tilly, K. H. de Grys, R. M. Myers, "Hall Thruster-Cathode Coupling," AIAA-1999-2865, 35th Joint Propulsion Conference, Los Angeles, CA, June 20-24, 1999.

[5]J. D. Sommerville, L. B. King, "Effect of Cathode position on Hall-Effect Thruster Performance and Cathode Coupling Voltage", AIAA-2007-5174, 43rd Joint Propulsion Conference, Cincinnati, OH, July 8-11, 2007.

[6]L. Albarède, V. Lago, P. Lasgorceix, M. Dudeck, A. Burgova, K. Malik, "Interaction of a Hollow Cathode Stream with a Hall Thurster", IEPC-2003-333, 28thInternational Electric Propulsion Conference, Toulouse, France, March 17-21, 2003.

[7]R. R. Hofer, L. K. Johnson, D. M. Goebel, and D. J. Fitzgerald, "Effects of an internally-mounted cathode on Hall thruster plume properties", AIAA-2006-4482, 42nd Joint Propulsion Conference, Sacramento, CA, July 9–12, 2006.

[8]R. R. Hofer and A. D. Gallimore, "Recent Results from Internal and Very-Near-Field Plasma Diagnostics of a High Specific Impulse Hall Thruster," IEPC-2003-037, 28th International Electric Propulsion Conference, Toulouse, France , March 17–21, 2003.

[9]M. L. Walker and A. D. Gallimore, "Hall Thruster Cluster Operation with a Shared Cathode," Journal of Propulsion and Power, Vol. 23, No. 3, 2007, pp. 528-536.

[10]J.R. Brophy, J.W. Barnett, J.M. Sankovic, and D.A. Barnhart, "Performance of the Stationary Plasma Thruster: SPT-100,", AIAA-92-3155, 28th Joint Propulsion Conference, Nashville, TN, July 6-8, 1992.

[11]V. Kim, "Main Physical Features and Processes Determining the Performance of Stationary Plasma Thrusters," Journal of Propulsion and Power, 14, No. 5, p. 736-743 (1998)

[12]A. Sengupta, J. Brophy, K. Goodfellow, "Status of the Extended Lift Test of the Deep Space 1 Flight Spare Ion Engine After 30'352 Hours of Operation", AIAA-2003-4558, 39th Joint Propulsion Conference, Huntsville, AL, July 20-23, 2003.

[13]D. M. Goebel and R. M. Watkins, "LaB_6 Hollow cathodes for Ion and Hall Thrusters", AIAA-2005-4239, 42nd Joint Propulsion Conference, Tucson, AZ, July 10-13, 2005.

[14] R. L. Seliger, "ExB Mass-Separator Design," Journal of Applied Physics, Vol. 43, No. 5, 1972.

[15] S. W. Kim and A. D. Gallimore, "Plume Study of a 1.35-kW SPT-100 Using an ExB Probe," Journal of Spacecraft and Rockets, Vol. 39, No. 6, 2002, pp. 904-909.

[16]A. Sengupta, J. Brophy, J. Anderson, C. Garner, "An Overview of the Results from the 30,000 Hr Life Test of the Deep Space 1 Flight Spare Ion Engine," AIAA-2004-3608, 40th Joint Propulsion Conference, Ft. Lauderdale, FL, July 11-14, 2004.

[17]J. E. Polk, J. R. Anderson, J. R. Brophy, "An Overview of the Results from an 8200 Hour Wear Test of the NSTAR Ion Thruster", AIAA-1999-2446, 35th Joint Propulsion Conference, Los Angeles, CA, June 20-24, 1999.

[18]D. M. Goebel and I. Katz, *Fundamentals of Electric Propulsion: Ion and Hall Thrusters*, John Wiley & Sons, NY, 2007.

[19]Brown, D. L., Larson, C. W., Haas, J. M., Gallimore, A. D., "Analytical Extraction of Plasma Properties Using a Hall Thruster Efficiency Architecture," IEPC-2007-188, 30th International Electric Propulsion Conference, Florence, Italy, September 17-20, 2007.

[20]Reid, B. M., Gallimore, A. D., Personal Communication, May 2007.

[21]T. B. Smith, "Deconvolution of Ion Velocity Distributions from Laser-Induced Fluorescnce Spectra of Xenon Electrostatic Thruster Plumes," dissertation, University of Michigan, 2003.

[22]D.M. Goebel, K. Jameson, I. Katz and I. Mikellides, "Plasma Potential Behavior and Plume Mode Transitions in Hollow Cathode Discharges" IEPC-2007-27, 30th International Electric Propulsion Conference, Florence, Italy, Sept. 17-20, 2007.

[23]I. Katz, R. R. Hofer, D. M. Goebel, "Ion Current in Hall Thrusters," IEPC-2007-365, 30thInternational Electric Propulsion Conference, Florence, Italy, September 17-20, 2007.

[24]I. G. Mikellides and I. Katz, "Numerical Simulations of a Hall Thruster Hollow Cathode Plasma," IEPC-2007-018, 30th International Electric Propulsion Conference, Florence, Italy, September 17-20, 2007.

[25]Mikellides, I. Katz, D. Goebel, K. Jameson and J. Polk, "Partially-Ionized Gas and Associated Wear in Electron Sources for Ion Propulsion, II: Discharge Hollow Cathode", AIAA-2007-5192, 43rd Joint Propulsion Conference, Cincinnati, OH, July 8-11, 2007.